1D-model of the interaction between a stack of wood and an imposed electromagnetic wave

Linus Hägg, Daniel Noreland,
Eddie Wadbro, and Martin Berggren

Abstract

We have developed and investigated a 1D-model for the interaction between a stack of wood and an impinging electromagnetic field. Maxwell's equations are used to model the electromagnetic interaction and each layer in a stack of boards has been modeled as a homogenous lossy dielectric slab.

The main reason for developing this model has been to investigate the possibility of measuring the moisture content of wood inside a drying kiln using electromagnetic waves.

Our investigations show that it is in principle possible to measure the moisture content, since the electromagnetic field is sensitive to changes in the moisture content of the wood. We also show that it might be possible to measure the average moisture content, without detailed knowledge of the distribution of moisture content between different boards.

Contents

1 Introduction

The moisture content of a piece of wood is defined as the ratio between the mass of the water it contains and its dry mass. Today, industrially sawn wood is dried in large chambers called kilns in order to lower the wood's moisture content to a pre-specified value. Kiln drying has many beneficial effects; for instance, both the resistance to biodegradation and the strength of the wood increase.

The drying process uses vast amounts of energy, mainly in terms of biofuel for heating of the kiln, but also in the form of electricity for the fans. A badly controlled drying process might lead to substantial quality and value loss.

For operating purposes, accurate measurements of the average moisture content of wood inside a drying kiln would be very valuable. The idea to use electromagnetic properties of the wood to determine the moisture content originates from the late 1920s [1], and hand held resistive moisture meters are widely used in industry today. To obtain satisfactory estimates of the average moisture content of a larger batch of wood by resistive meters is however cumbersome, since they only provide very localized measurements. Neither are the resistive meters suitable for continuously measuring the moisture content since they rely on adequate contact between the wood and the electrodes.

To investigate the possibility of in kiln moisture content measurements, we have developed a simplified model of the interaction between an imposed electromagnetic field and a stack of wood. This report is however mainly devoted to describe the aforementioned 1D-model and not on how to extract the moisture content based on electromagnetic measurements. We will begin by presenting some preliminary electrodynamics[1], which will be used in consequent chapters to develop and exploit the model.

2 Preliminary electrodynamics

Maxwell's equations govern the electromagnetic field and its interaction with matter, and in the case of a linear homogenous and isotropic Ohmic conductor they are given by

$$\nabla \cdot E = 0, \tag{1}$$

$$\nabla \cdot B = 0, \tag{2}$$

$$\nabla \times E = -\frac{\partial B}{\partial t}, \tag{3}$$

$$\nabla \times B = \mu\epsilon\frac{\partial E}{\partial t} + \mu\sigma E, \tag{4}$$

where $\mu = \mu_r\mu_0$ is the permeability, $\epsilon = \epsilon_r\epsilon_0$ is the permittivity, and σ is the conductivity of the medium. These equations admit plane wave solutions, and by aligning the coordinate system, these can be taken to be proportional to $e^{i(kz-\omega t)}$, where $\pm z$ are coordinates in the propagation direction, k is the (complex) wave number, and ω is the (real) angular frequency. We will hence use the ansatz

$$E = E_0 e^{i(kz-\omega t)}\hat{x}, \tag{5}$$

$$B = B_0 e^{i(kz-\omega t)}\hat{y}, \tag{6}$$

where E_0 and B_0 are complex amplitudes of the electric and magnetic fields respectively, and $\hat{x}$ and $\hat{y}$ are unit vectors along the x and y axis respectively. It is easily verified that this ansatz satisfies the first two of Maxwell's equations, equation (1) and equation (2), while the third, equation (3) yields the following relation between the field amplitudes

$$B_0 = \frac{k}{\omega}E_0. \tag{7}$$

Insertion of the ansatz and equation (7) into the fourth Maxwell equation (4) yields the dispersion relation

$$k^2 = \mu\epsilon\omega^2\left(1 + i\tan\delta\right), \tag{8}$$

[1] A more comprehensive account on electrodynamics can be found in, for instance, [2].

where we have introduced the loss tangent

$$\tan\delta = \frac{\sigma}{\epsilon\omega}. \tag{9}$$

The expression

$$\pm\sqrt{w} = \sqrt{a}\left[\frac{\sqrt{1+b^2}+1}{2}\right]^{1/2} + i\sqrt{a}\left[\frac{\sqrt{1+b^2}-1}{2}\right]^{1/2} \tag{10}$$

for the square root of a complex number $w = a\,(1+ib)$ with $a, b \geq 0$ applied on equation (8) gives

$$k = \pm k_0\,(a_+ + ia_-)\,, \tag{11}$$

$$a_\pm = \sqrt{\epsilon_r\mu_r}\left[\frac{\sqrt{1+\tan^2\delta}\pm 1}{2}\right]^{1/2} \geq 0, \tag{12}$$

were $k_0 = \omega\sqrt{\epsilon_0\mu_0}$ is the wave number in vacuum; the positive sign in expression (11) corresponds to a wave propagating along the positive z axis, while the negative sign corresponds to propagation along the negative z axis. Since Maxwell's equations are linear, a general monochromatic plane wave solution representing waves propagating along both the positive and negative z axis is given by

$$E = \left[E^+e^{ikz} + E^-e^{-ikz}\right]e^{-i\omega t}\hat{x}, \tag{13}$$

$$B = \frac{k}{\omega}\left[E^+e^{ikz} - E^-e^{-ikz}\right]e^{-i\omega t}\hat{y}, \tag{14}$$

where $E^\pm$ are the complex amplitudes of the electric field and where we have used expression (7) to eliminate the corresponding amplitudes of the magnetic field.

The Poynting vector Y determines the energy flux density, and its time average can in the case of expressions (13) and (14) be calculated as

$$\langle Y\rangle = \frac{1}{2}\mathrm{Re}\left(E^* \times \frac{B}{\mu}\right) \tag{15}$$

$$= \left[\frac{\mathrm{Re}(k)}{2\mu\omega}\left(|E^+|^2 - |E^-|^2\right) + \frac{\mathrm{Im}(k)}{\mu\omega}\mathrm{Im}\left(E^-E^{+*}\right)\right]\hat{z}, \tag{16}$$

where * denotes complex conjugation.

3 Scattering by one linear slab

In this section, we study how a linear, homogenous, lossy dielectric slab scatters a monochromatic plane electromagnetic wave at normal incidence. The setup is illustrated in figure 1 where we also show the definitions of the complex amplitudes $E_l^\pm$ of the electric field in the different regions $l \in \{L, M, R\}$; $E_L^\pm$ is defined in region L at the interface between regions L and M; $E_M^\pm$ is defined in region M at the interface between regions L and M; $E_R^\pm$ is defined in region R at the interface between regions M and R. We will use a transfer matrix method[2] to relate the amplitudes in the different regions [3]. In our application, the material in regions L and R will be the same and it will also be assumed that the material in these regions is lossless; that is, $\tan\delta_L = \tan\delta_R = 0$.

[2]Transfer matrix methods are also used for analyzing acoustical and quantum mechanical wave scattering.

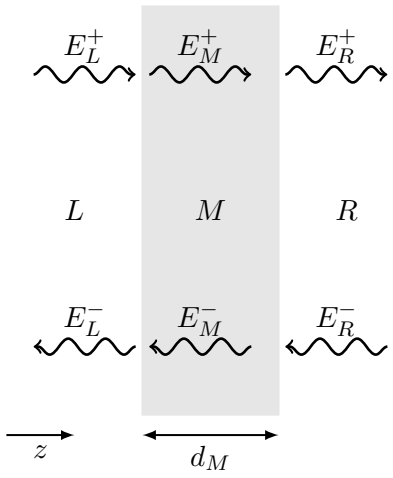

Figure 1: Definitions of the notation used for the six complex amplitudes related to the dielectric slab.

At the interface between two regions with different material properties, the electric and magnetic field must satisfy so-called interface conditions; in this particular case that the electric field and the H-field $H = \frac{1}{\mu}B$ should be continuous at the interface. The interface conditions for the fields at the LM-interface can be summarized as

$$C_L \begin{pmatrix} E_L^+ \\ E_L^- \end{pmatrix} = C_M \begin{pmatrix} E_M^+ \\ E_M^- \end{pmatrix}, \tag{17}$$

where the first component corresponds to the electric field and the second to the H-field. At the MR-interface the corresponding interface conditions are given by

$$C_M P_M \begin{pmatrix} E_M^+ \\ E_M^- \end{pmatrix} = C_R \begin{pmatrix} E_R^+ \\ E_R^- \end{pmatrix} \tag{18}$$

In equations (17) and (18) the connection matrices C_l, $l \in \{L, M, R\}$ are defined as

$$C_l = \begin{pmatrix} 1 & 1 \\ a_l & -a_l \end{pmatrix}, \tag{19}$$

where $a_l \equiv k_l/\mu_l$, and the propagation matrix P_l is defined as

$$P_l = \begin{pmatrix} e^{ik_l d_l} & 0 \\ 0 & e^{-ik_l d_l} \end{pmatrix} \equiv \begin{pmatrix} \varphi_l & 0 \\ 0 & \varphi_l^{-1} \end{pmatrix}. \tag{20}$$

Note that since $k_l \in \mathbb{C}$ we have, in general, that $\varphi_l^{-1} \neq \varphi_l^*$.

Solving for $E_R^\pm$ in terms of $E_L^\pm$ gives

$$\begin{pmatrix} E_R^+ \\ E_R^- \end{pmatrix} = T \begin{pmatrix} E_L^+ \\ E_L^- \end{pmatrix}, \tag{21}$$

where we have defined the transfer matrix $T = C_R^{-1} C_M P_M C_M^{-1} C_L$. Since $C_L = C_R$, T is related to P_M via a similarity transformation and hence

$$\det(T) = \det(P_M) = 1, \tag{22}$$

where the last equality follows from expression (20).

By definition (19) it follows that

$$C_L^{-1}C_M = \frac{1}{1-q}\begin{pmatrix} 1 & -q \\ -q & 1 \end{pmatrix}, \tag{23}$$

where $q \equiv \Delta a / \sum a$, $\sum a \equiv a_L + a_M$, and $\Delta a \equiv a_M - a_L$. The matrix $C_M^{-1}C_L$ is found from expression (23) by interchanging L and M noticing that $\sum a \to \sum a$, and $\Delta a \to -\Delta a$, and hence $q \to -q$. Using these observations the entries of T can be computed as

$$T = \frac{\varphi_M^{-1}}{1-q^2}\begin{pmatrix} \varphi_M^2 - q^2 & -q(1-\varphi_M^2) \\ q(1-\varphi_M^2) & 1-q^2\varphi_M^2 \end{pmatrix}. \tag{24}$$

We note that if $\mathrm{Im}(k_M)d_M \gg 1$, that is, if the losses in M are large or the slab is thick, the entries of T will be very large. Hence T is not suitable for computations using finite precision arithmetic, and it is preferable to work with the scattering matrix S instead, defined via

$$\begin{pmatrix} E_L^- \\ E_R^+ \end{pmatrix} = S \begin{pmatrix} E_L^+ \\ E_R^- \end{pmatrix}. \tag{25}$$

By rearranging the terms of equation (21) in accordance with equation (25) we find that

$$S_{11} = -\frac{T_{21}}{T_{22}}, \tag{26}$$

$$S_{12} = \frac{1}{T_{22}}, \tag{27}$$

$$S_{21} = \frac{\det(T)}{T_{22}} \overset{(22)}{=} \frac{1}{T_{22}}, \tag{28}$$

$$S_{22} = \frac{T_{12}}{T_{22}}. \tag{29}$$

We see that $S_{12} = S_{21}$ and by equation (24) that $S_{11} = S_{22}$ since $T_{12} = -T_{21}$. These symmetries of the scattering matrix are anticipated due to the symmetry of the problem. By rearranging the terms in definition (25) we find that

$$\begin{pmatrix} E_R^+ \\ E_L^- \end{pmatrix} = PSP \begin{pmatrix} E_R^- \\ E_L^+ \end{pmatrix}, \tag{30}$$

where $P = P^{-1} = \left(\begin{smallmatrix} 0 & 1 \\ 1 & 0 \end{smallmatrix}\right)$, but since the problem is symmetric the relation between ingoing and outgoing waves must be invariant, meaning that $S = PSP$. Hence we must have $S_{11} = S_{22}$ and $S_{12} = S_{21}$ which according to expression (26) to (29) means that we must have $\det(T) = 1$ and $T_{12} = -T_{21}$. We remark that systems with the property $S_{12} = S_{21}$ are called reciprocal, see for instance [4].

From equation (24) and equations (26) to (29) we finally get

$$S_{11} = S_{22} = -\left(\frac{1-\varphi_M^2}{1-q^2\varphi_M^2}\right) q, \tag{31}$$

$$S_{12} = S_{21} = \left(\frac{1-q^2}{1-q^2\varphi_M^2}\right) \varphi_M. \tag{32}$$

We note that the entries of S remain finite even when $\mathrm{Im}(k_M)d_M \gg 1$

Figure 2: An array of five consecutive slabs.

4 Scattering by N linear slabs

In this section we extend the results from the previous section to an array of N consecutive slabs at normal incidence, see figure 2. Parenthesized superscripts will be used to indicate which slab the corresponding quantity is related. We note that

$$\begin{pmatrix} E^+_{L,n+1} \\ E^-_{L,n+1} \end{pmatrix} = P^{(n)}_R \begin{pmatrix} E^+_{R,n} \\ E^-_{R,n} \end{pmatrix}, \tag{33}$$

that is, the field to the left of slab $n+1$ can be obtained by propagating the field to the right of slab n. By equation (21), we furthermore get that the global transfer matrix T_G is found by multiplying the elemental transmission matrices:

$$\begin{pmatrix} E^+_{R,N} \\ E^-_{R,N} \end{pmatrix} = {P^{(N)}_R}^{-1} \left(\prod_{j=1}^{N} P^{(j)}_R T^{(j)} \right) \begin{pmatrix} E^+_{L,1} \\ E^-_{L,1} \end{pmatrix} \equiv T_G \begin{pmatrix} E^+_{L,1} \\ E^-_{L,1} \end{pmatrix} \tag{34}$$

Despite being easy to compute the global transfer matrix in (34) suffers from the same behavior as its elemental counterpart when there are losses present, that is, the elements of T_G can be very large. As pointed out before, elemental scattering matrices do not suffer from that behavior and can be related to the global scattering matrix S_G defined via

$$\begin{pmatrix} E^-_{L,1} \\ E^+_{R,N} \end{pmatrix} = S_G \begin{pmatrix} E^+_{L,1} \\ E^-_{R,N} \end{pmatrix}. \tag{35}$$

We remark that S_G is related to T_G in the same way as S is related to T, see expression (26) to (29), and that we still have $\det(T_G) = 1$. However, in general, $T_{G12} \neq -T_{G21}$ which means that $S_{G12} = S_{G21}$ but $S_{G11} \neq S_{G22}$. If the array is symmetric with respect to the center plane we will however still have $PS_GP = S_G$ as for the elemental scattering matrix S.

Defining $E^{(n)} \in \mathbb{C}^4$ as

$$E^{(n)} = \begin{pmatrix} E^+_{L,n} & E^-_{R,n} & E^-_{L,n} & E^+_{R,n} \end{pmatrix}^T, \tag{36}$$

$G^{(n)} \in \mathbb{C}^{4\times 8}$ as

$$G^{(n)} = \begin{pmatrix} G_{11}^{(n)} & G_{12}^{(n)} \\ G_{21}^{(n)} & G_{22}^{(n)} \end{pmatrix} \tag{37}$$

where

$$G_{11}^{(n)} = \begin{pmatrix} S^{(n)} & -I \end{pmatrix} \in \mathbb{C}^{2\times 4} \tag{38}$$

$$G_{12}^{(n)} = \begin{pmatrix} 0 & 0 & 0 & 0 \\ 0 & 0 & 0 & 0 \end{pmatrix} \tag{39}$$

$$G_{21}^{(n)} = \begin{pmatrix} 0 & 0 & 0 & \varphi_R^{(n)} \\ 0 & 1/\varphi_R^{(n)} & 0 & 0 \end{pmatrix} \tag{40}$$

$$G_{22}^{(n)} = \begin{pmatrix} -1 & 0 & 0 & 0 \\ 0 & 0 & -1 & 0 \end{pmatrix} \tag{41}$$

the problem of finding the complex amplitudes of the electric field boils down to solving $Ax = b$ for $x = (E^{(1)T}, \ldots, E^{(N)T})^T$ where

$$A = \left(\begin{array}{ccc} G^{(1)} & & 0 \\ & \ddots & \\ 0 & & G_{11}^{(N)} \\ \hline & \text{BC} & \end{array}\right), b = \left(\begin{array}{c} 0 \\ \vdots \\ 0 \\ \hline \text{bc} \end{array}\right). \tag{42}$$

The parts BC and bc are used to enforce boundary conditions at the first and last slab. The boundary conditions we have used are

$$E_{L,1}^{+} = E_I \tag{43}$$

$$E_{R,N}^{-} = \xi E_{R,N}^{+}, \tag{44}$$

where E_I is the amplitude of an incoming wave and $\xi \in \mathbb{C}$, $|\xi| \leq 1$ is a constant that can be adjusted to generate different boundary conditions. For instance $\xi = 0$ corresponds to the case when nothing is reflected at the far end while $\xi = -1$ corresponds to ending the array with a perfect electric conductor. Note that the condition $|\xi| \leq 1$ guarantees that no energy is gained at the boundary.

The reflection coefficient r_ξ is defined as the quotient of the amplitude of the reflected wave and that of the incident wave:

$$r_\xi = \frac{E_{L,1}^{-}}{E_{L,1}^{+}} \tag{45}$$

Similarly the transmission coefficient t_ξ is defined as the quotient of the amplitude of the transmitted wave and that of the incident wave:

$$t_\xi = \frac{E_{R,N}^{+}}{E_{L,1}^{+}} \tag{46}$$

Using the boundary conditions (43) and (44) in expression (35) the reflection and transmission coefficients can be computed as

$$r_\xi = r_0 + t_0' \xi t_\xi, \tag{47}$$

$$t_\xi = t_0 + r_0' \xi t_\xi \Leftrightarrow t_\xi = \frac{t_0}{1 - \xi r_0'}, \tag{48}$$

where $r_0 = S_{G11}$ and $t_0 = S_{G21}$ are the reflection and transmission coefficients respectively when $\xi = 0$, and $r'_0 = S_{G22}$ and $t'_0 = S_{G12}$ are the reflection and transmission coefficients respectively for the same array, but with the boundary conditions:

$$E^+_{L,1} = 0 \tag{49}$$

$$E^-_{R,N} = E_I, \tag{50}$$

Note that $\xi r'_0 = 1$ if and only if $|\xi| = |r'_0| = 1$, which implies that $t'_0 = 0$ since energy balance demands that $|r'_0|^2 + |t'_0|^2 \leq 1$. A remarkable property for any type of system with $\det(T_G) = 1$, as for instance the type of arrays studied here, is that $t'_0 = t_0$ since $S_{G12} = S_{G21}$.

The input impedance Z is defined as the quotient of the electric and magnetic field and is given by

$$Z = \eta \frac{1 + r_\xi}{1 - r_\xi}, \tag{51}$$

where $\eta = \mu_0 c$ is the impedance of vacuum. Z can be used to quantify the response of a system to an imposed electromagnetic wave.

4.1 Analytic solution

Assuming all unit cells to be equal (hence the array is symmetric with respect to the center plane) we get from equation (34) that the global transfer matrix is given by

$$T_G = P_R^{-1} \left(P_R T\right)^N. \tag{52}$$

Using the results in Appendix A on page 13 we get (note that $\det(P_R T) = 1$)

$$(P_R T)^n = \frac{\sin n\theta}{\sin\theta} P_R T - \frac{\sin(n-1)\theta}{\sin\theta} I \Rightarrow \tag{53}$$

$$T_G = \frac{\sin n\theta}{\sin\theta} T - \frac{\sin(n-1)\theta}{\sin\theta} P_R^{-1}, \tag{54}$$

where $\cos\theta = \mathrm{tr}(P_R T)/2$. Using equation (24) we get

$$\cos\theta = \frac{1}{1-q^2}\left[\cos(k_R d_R + k_M d_M) - q^2 \cos(k_R d_R - k_M d_M)\right] \tag{55}$$

Hence we get the following explicit expressions for the entries of S_G

$$S_{G11} = S_{G22} = S_{11} \frac{g_n(\theta)}{g_n(\theta) - S_{12} g_{n-1}(\theta) \varphi_R e^{i\theta}} \tag{56}$$

$$S_{G12} = S_{G21} = S_{12} \frac{g_1(\theta) e^{i(n-1)\theta}}{g_n(\theta) - S_{12} g_{n-1}(\theta) \varphi_R e^{i\theta}}, \tag{57}$$

where $g_n(\theta) \equiv 2ie^{in\theta} \sin n\theta = e^{i2n\theta} - 1$.

The analysis in this section show that the response of the array to an imposed electromagnetic field in general depends in a complex way on the material properties and geometry.

5 Simulation results

To verify the model in the lossless case we tested energy conservation by computing

$$\delta = |\mathcal{R} + \mathcal{T} - 1|, \tag{58}$$

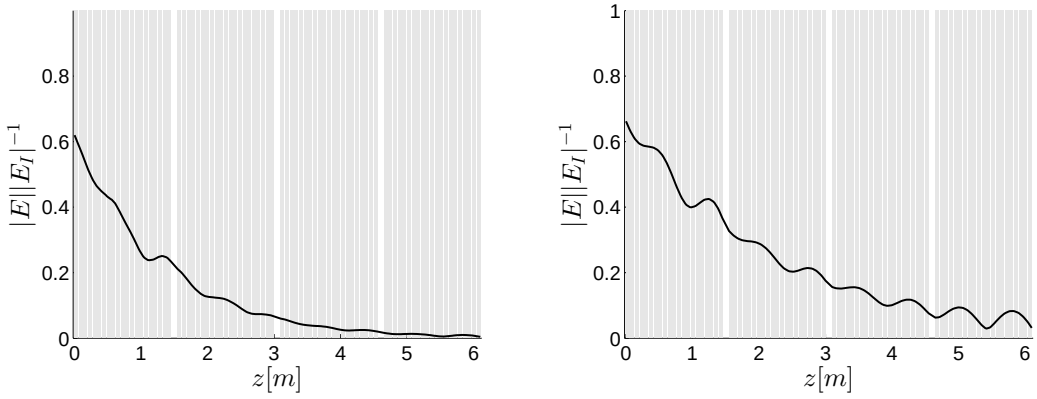

(a) $u = 30\,\%$ (b) $u = 20\,\%$

Figure 3: Electric field in a pile of wood consisting of four packages containing 21 boards with thickness 50 mm and moisture content u when hit by a wave with frequency 100 MHz.

where $\mathcal{R} = |r_0|^2$ is the reflectance and $\mathcal{T} = |t_0|^2$ is the transmittance. We found that $\max_\nu \delta \sim 10^{-12}$. In the lossy case we used equation (15) to test that the energy flux out of each slab was less than the corresponding influx. We have also compared the numerical solution with the analytic expressions in section 4.1.

The model has been tested on a stack of wood consisting of 84 boards distributed in four packages with 21 boards each. Each board was 50 mm thick and the air gaps between boards in a package was 20 mm and the air gap between two consecutive packages was 100 mm. This means that the stack will be about 6 m high in total. At the far end of the stack we used a boundary condition that tries to mimic the effect of a 100 mm air gap followed by reinforced concrete by choosing ξ in equation (43).

For the properties of wood at different moisture contents and frequencies we used the values tabulated in [5]. For intermediate frequencies not found in the table we interpolated linearly between the entries in the table.

Figure 3a shows the magnitude of the electric field inside a stack of wood with moisture content 30 % at 100 MHz. It can be seen that the behavior is dominated by the damping even though some interference is also present. Figure 3b shows the corresponding figure for $u = 20\,\%$. The damping is still dominating the behavior but now the interference is more pronounced. For higher moisture contents the field is practically damped out already in the first package. Due to the low penetration at high moisture contents we will henceforth assume that the pile has been partitioned after the first package using a metallic mesh. This means that the response computed only depends on the properties of the first package.

Figure 4 shows the input impedance as a function of frequency for a package with average moisture content 100 %. The thicker line shows the response when there is no variation in moisture content between different boards in the package while the four thinner shows the response when there is 50 % variation. We see that all five curves shows a high degree of agreement up to around 30 MHz. This means that the response for low frequencies is mainly due to the average properties of the package and not the variation. This is expected since the low frequency limit corresponds to the long wavelength limit. When the wavelength is much larger than the thickness of the boards in the package, the package can be approximated with a homogenous block with some effective electromagnetic properties.

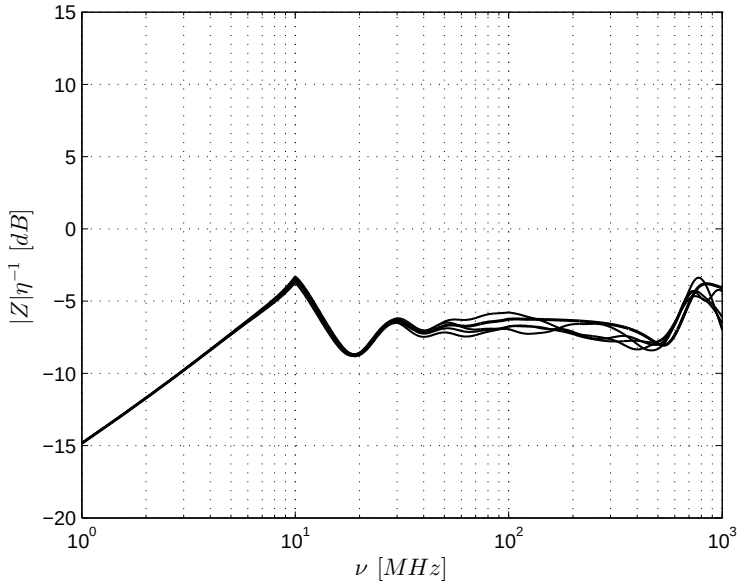

Figure 4: Input impedance for a package of wood ended by a perfect electric conductor. The thicker line shows the response when all slabs have moisture content 100 %. The four thinner ones correspond to cases where the moisture content varies between different slabs but the average moisture content of the package is still 100 %.

The figures 5a, 5b, 5c and 5d shows to figure 4 corresponding figures when the moisture content is 60, 30, 20 % and 10 % respectively. These figures show the same general tendency as figure 4, that is for low frequencies the response is mainly due to the average properties of the package. However what is regarded as a low frequency changes with the average moisture content.

6 Conclusion

Our investigations show that the electromagnetic field is sensitive to changes in moisture content of a pile of wood. At high moisture contents the penetration is quite poor and the behavior of the electromagnetic field inside the pile is mainly characterized by exponential damping. For lower moisture contents, when there is less damping, interference effects are also present. The response for low frequencies is mainly related to the average electromagnetic properties of the pile. This indicates that it should be possible to measure the average moisture content of the wood without detailed knowledge of the distribution of moisture content between different boards.

The model presented in this report neglects all 3D-effects, as for instance the finite size of the packages and non normal propagation of the electromagnetic waves. Within this project these effects have not been studied.

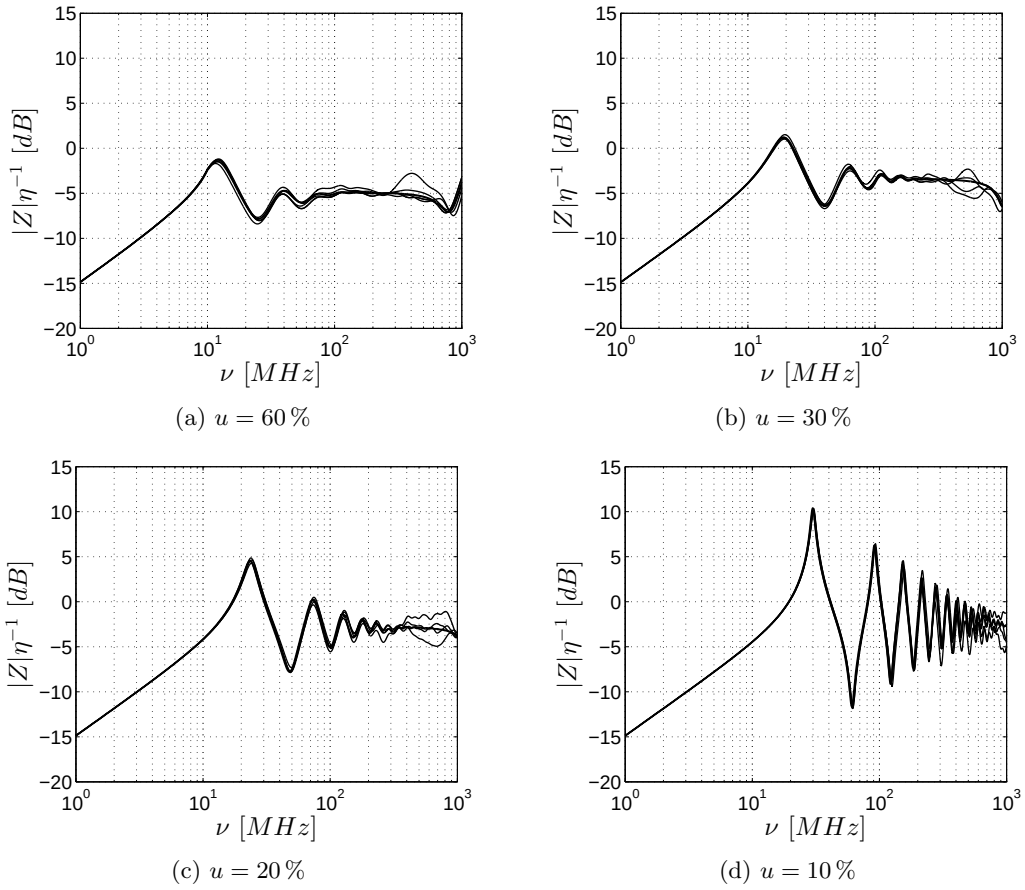

(a) $u = 60\,\%$ (b) $u = 30\,\%$

(c) $u = 20\,\%$ (d) $u = 10\,\%$

Figure 5: Input impedance for a package of wood ended by a perfect electric conductor. The thicker line shows the response when all slabs have moisture content u. The four thinner ones correspond to cases where the moisture content varies between different slabs but the average moisture content of the package is still u.

A Powers of a 2×2 matrix

Let $M \in \mathbb{R}^{2\times 2}$ then

$$M^0 = I \tag{59}$$
$$M^1 = M \tag{60}$$
$$M^2 = \mathrm{tr}(M)M - \det(M)I \equiv \alpha M + \beta I \tag{61}$$

where equation (61) follows by brute force or the Cayley-Hamilton theorem. The sequence of powers shows that $M^n = a_n M + b_n I$ for some a_n and b_n. Using this as an ansatz we get

$$\begin{aligned} a_{n+1}M - b_{n+1}I &= M^{n+1} && (62)\\ &= M(a_n M + b_n I) && (63)\\ &= a_n M^2 + b_n M && (64)\\ &= a_n(\alpha M + \beta I) + b_n M && (65)\\ &= (\alpha a_n + b_n)M + \beta a_n I && (66) \end{aligned}$$

ie. $a_{n+1} = \alpha a_n + b_n$ and $b_{n+1} = \beta a_n$ which together with equation (59) and (60) yields the following recurrence relation:

$$\begin{aligned} a_0 &= 0\\ a_1 &= 1\\ a_n &= \alpha a_{n-1} + \beta a_{n-2} \end{aligned} \tag{67}$$

Define the operator S by $Sa_n = a_{n+1}$ then the recurrence can be written as

$$(S^2 - \alpha S - \beta)a_n = 0 \tag{68}$$

which factors into $(S - \lambda_1)(S - \lambda_2)a_n = 0$ where λ_i is the i:th eigenvalue of M. We will assume that $\lambda_1 \neq \lambda_2$. Hence $a_n = A_1\lambda_1^n + A_2\lambda_2^n$ is a solution to the recurrence (67) for any pair of constants A_i. Further since the recurrence is homogenous this is also the only solution. Using that $a_0 = 0$ and $a_1 = 1$ we get finally that $A_1 = -A_2 = 1/(\lambda_1 - \lambda_2)$ and hence:

$$a_n = \frac{\lambda_1^n - \lambda_2^n}{\lambda_1 - \lambda_2} \tag{69}$$

For a matrix with $\det(M) = 1$ we get that $\lambda_1 = 1/\lambda_2 \equiv e^{i\theta}$, $\mathrm{tr}(M) = \lambda_1 + \lambda_2 = e^{i\theta} + e^{-i\theta} = 2\cos\theta$ and that $a_n = \sin n\theta / \sin\theta$, *note that* $\theta \in \mathbb{C}$. Hence the nth power of M is given by:

$$M^n = a_n M - \det M a_{n-1} I = \frac{\sin n\theta}{\sin\theta} M - \frac{\sin(n-1)\theta}{\sin\theta} I \tag{70}$$

References

[1] A. J. Stamm (1927). *The electrical resistance of wood as a measure of its moisture content*, Industrial and Engineering Chemistry 19(9): 1021-1025.

[2] D. J. Griffiths (2004). *Introduction to electrodynamics*, 3rd ed, Pearson Education.

[3] S. J. Orfanidis (2014). *Electromagnetic waves and antennas*, online at `http://www.ece.rutgers.edu/~orfanidi/ewa/`

[4] D. M. Pozar (2011). *Microwave Engineering*, 4th ed, Ch. 4, John Wiley & Sons

[5] G. I. Torgovnikov (1993). *Dielectric properties of wood and wood-based materials*, Springer Series in Wood Science, Springer-Verlag, Berlin.